Interaction of two spherical elastic waves in a nonlinear five-constant medium

Igor A. Beresnev[a)]
Institute of Physics of the Earth, Russian Academy of Sciences, Bolshaya Gruzinskaya 10, Moscow 123810, Russia

(Received 15 September 1992; accepted for publication 19 July 1993)

The interaction of two spherical longitudinal waves produced by noncoincident sources with the generation of a transverse difference-frequency wave is studied theoretically. The equation of motion from five-constant elasticity theory to the second order in the displacement is used as a mathematical model. The general solution for the difference-frequency field outside the wave interaction region is obtained in the form of a scattering integral. An analytical solution for plane intersecting beams is derived as a limit case of small interaction volumes. For the general case, the solution is analyzed numerically, and the effect of the sphericity of interacting waves is compared with the results of plane-wave resonance interaction. In the limit of large interaction volumes, backscattering at the difference frequency is formed. This effect suggests the use of this type of nonlinear interaction for remote sensing of the nonlinear properties of the Earth's crust.

PACS numbers: 43.25.Lj

INTRODUCTION

Nonlinear interactions of noncollinear plane wave sound beams have been studied theoretically in a number of publications.[1-3] Selection rules have been established that determined the conditions for resonance interactions (the so-called "synchronism" conditions), under which directed beams of sum and difference-frequency waves were formed. Synchronism conditions define the relationship between frequencies of interacting waves and compressional and shear wave velocities for which the resonance interaction is possible; the angle of a scattered wave can be found from these conditions for given frequency and velocity ratios.[1] These selection rules for the scattering of sound by sound in solids (combination scattering) have been validated experimentally in several works.[4-7]

Recently the use of combination scattering of seismic waves to measure the earth's crust nonlinear coefficients has been proposed.[8] The nonlinear coefficient of rock may provide important information about its mechanical conditions, porosity, the presence of microcracks, etc.[6,9-12]

However, seismic waves excited by point-like surface-based sources spread spherically, making the theory of interacting plane beams of limited applicability to seismology. Spherical spreading also makes interactions intrinsically nonresonant. A theory of the interaction of spherical longitudinal waves produced by noncoincident sources is developed in this paper.

I. THEORY

We assume that two point sources O_1 and O_2 of longitudinal elastic waves are located in a homogeneous and isotropic elastic solid at some distance from each other. They radiate continuous sinusoidal waves with frequencies f_1 and f_2, respectively. We also assume that the interaction of these waves takes place in a limited spatial region (Fig. 1). Elastic motion of the medium will be described by the equations of a five-constant elasticity theory.[1,13,14] For simplicity, the generation of only the difference-frequency wave (DFW) will be considered.

Let us write the equation of motion of a five-constant theory to the second order in the displacement:

$$\rho_0\frac{\partial^2 u_i^{(s)}}{\partial t^2}-\mu\frac{\partial^2 u_i^{(s)}}{\partial x_k^2}-\left(K+\frac{\mu}{3}\right)\frac{\partial^2 u_l^{(s)}}{\partial x_l\,\partial x_i}$$
$$=\left(\mu+\frac{A}{4}\right)\left(\frac{\partial^2 u_l}{\partial x_k^2}\frac{\partial u_l}{\partial x_i}+\frac{\partial^2 u_l}{\partial x_k^2}\frac{\partial u_i}{\partial x_l}+2\frac{\partial^2 u_i}{\partial x_l\,\partial x_k}\frac{\partial u_l}{\partial x_k}\right)$$
$$+\left(K+\frac{\mu}{3}+\frac{A}{4}+B\right)\left(\frac{\partial^2 u_l}{\partial x_i\,\partial x_k}\frac{\partial u_l}{\partial x_k}+\frac{\partial^2 u_k}{\partial x_l\,\partial x_k}\frac{\partial u_i}{\partial x_l}\right)$$
$$+\left(K-\frac{2}{3}\mu+B\right)\frac{\partial^2 u_i}{\partial x_k^2}\frac{\partial u_l}{\partial x_l}+\left(\frac{A}{4}+B\right)\left(\frac{\partial^2 u_k}{\partial x_l\,\partial x_k}\frac{\partial u_l}{\partial x_i}\right.$$
$$\left.+\frac{\partial^2 u_l}{\partial x_i\,\partial x_k}\frac{\partial u_k}{\partial x_l}\right)+(B+2C)\frac{\partial^2 u_k}{\partial x_i\,\partial x_k}\frac{\partial u_l}{\partial x_l},\qquad(1)$$

where $u_i^{(s)}$ is the ith component of the displacement in the scattered difference-frequency wave, u_i is the ith component of the primary waves, K and μ are second-order elastic moduli, and A, B, and C are third-order moduli.

Following Jones and Kobett's[1] approach, we will solve Eq. (1) using a Green's function method for an inhomogeneous wave equation. The right-hand side of Eq. (1) is a known function of primary waves. Using the designations of Fig. 1, the primary wave field can be represented as a vector sum of spherical longitudinal waves with the sources at points O_1 and O_2:

$$u_i=\frac{F_0}{2\pi\mu}\left(\frac{\mathbf{R}_1}{R_1^2}e^{i(k_1R_1-2\pi f_1 t)}+\frac{\mathbf{R}_2}{R_2^2}e^{i(k_2R_2-2\pi f_2 t)}\right)_i,\qquad(2)$$

[a)]Present address: Institute of Earth Sciences, Academia Sinica, P.O. Box 1-55, Nankang, Taipei, Taiwan 11529, R.O.C.

 0001-4966/93/94(6)/3400/5/$6.00

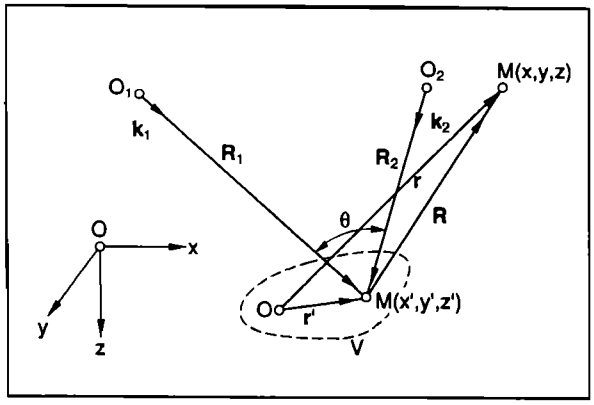

FIG. 1. Geometry of the problem. Here, O_1 and O_2 are sources of primary waves, $\mathbf{k}_1$ and $\mathbf{k}_2$ are their wave vectors, M is an observation point, M' is a point belonging to the interaction region, O is origin, V is the interaction region; $\mathbf{R}$, $\mathbf{R}_1$, $\mathbf{R}_2$, $\mathbf{r}$, $\mathbf{r}'$ are radius vectors. Directions of the axes of a Cartesian coordinate system are also shown.

where $R_{1,2}=|\mathbf{R}_{1,2}|$, F_0 is the force amplitude produced by the sources, μ is the shear modulus, and the subscript $_i$ in the right-hand side means the projection of a field on the i axis. We use in Eq. (2) the expression for the far field of piston sources in a solid[15] to make the formulas applicable to seismic exploration problems. We assume, therefore, that the interaction region is located in the far field of the sources, i.e., the conditions $k_{1,2}R_{1,2}\gg 1$ are satisfied. After we substitute expression (2) into the right-hand side of Eq. (1), and keep only terms with the difference frequency, the right-hand side becomes

$$p_i=(F_0^2/4\pi^2\mu^2)I_i\sin[2\pi(f_1-f_2)t-(k_1R_1-k_2R_2)], \tag{3}$$

where the amplitude factor I_i has the following components:

$$I_x=-\frac{1}{2}\frac{k_1k_2}{R_1R_2}\left[(x_1-L)\frac{k_2}{R_2}-x_1\frac{k_1}{R_1}\right][\cdots],$$

$$I_y=-\frac{y_1}{2}\frac{k_1k_2}{R_1R_2}\left(\frac{k_2}{R_2}-\frac{k_1}{R_1}\right)[\cdots],$$

$$I_z=-\frac{z_1}{2}\frac{k_1k_2}{R_1R_2}\left(\frac{k_2}{R_2}-\frac{k_1}{R_1}\right)[\cdots];$$

$$[\cdots]=[(K+\tfrac{7}{3}\mu+A+2B)\cos^2\theta+(K-\tfrac{2}{3}\mu+2B+2C)]; \tag{4}$$

x_1, y_1, and z_1 are coordinates of the vector $\mathbf{R}_1$ and L is the distance between the sources.

Applying a Fourier transform to Eq. (1) with a right-hand side defined by Eqs. (3) and (4), we find a vector Helmholtz equation, for which the exact form of a Green's (tensor) function is known.[1] Using this Green's function, we can obtain the solutions for both longitudinal and transverse scattered waves. We will confine ourselves to the transverse scattered wave solution, since in the plane wave case, only the transverse difference-frequency wave satisfies the resonance conditions,[1-3] when two longitudinal waves interact. In the following, we will compare the results of a resonance interaction of plane waves with the interaction of spherical waves, to infer how sphericity affects the scattered field.

Using the expression

$$u_i^{(s)}(r_i,2\pi f)=\int_V G_{ij}(r_i,r_i',2\pi f)p_j(r_i',2\pi f)dv, \tag{5}$$

where $G_{ij}(r_i,r_i',2\pi f)$ is the "transverse" part of a Green's tensor, $p_j(r_i',2\pi f)$ is the Fourier transform of the Eq. (3), and the integration is carried out over the interaction volume V, we obtain the frequency-domain solution for ith component of the scattered transverse wave field at the point M outside the interaction region (the superscript $^{(s)}$ is omitted below). Applying an inverse Fourier transform, we obtain the final solution in the time domain. For the x component of the scattered field, the solution is

$$u_x(r_i,t)=\frac{k_1k_2zF_0^2}{32\pi^2\mu^2}\int_V\frac{1}{K\_R^2}\frac{m\cos^2\theta+n}{R_1R_2}\left[\left(\frac{k_2}{R_2}-\frac{k_1}{R_1}\right)\times\left(\frac{1-K\_^2R^2}{K\_R}\sin\Psi+\cos\Psi\right)-\frac{1}{R^2}[\mathbf{R}(\mathbf{k}_2-\mathbf{k}_1)]\times\left(\frac{3-K\_^2R^2}{K\_R}\sin\Psi+\cos\Psi\right)\right]dv, \tag{6}$$

where $K\_$ is the DFW wave number, $m=K+7\mu/3+A+2B$, $n=K-2\mu/3+2B+2C$, $\mathbf{k}_{1,2}=k_{1,2}\mathbf{R}_{1,2}/R_{1,2}$; $\Psi=-k_1R_1+k_2R_2-2\pi(f_1-f_2)(R/c_t-t)$, and c_t is the shear wave velocity.

II. PLANE WAVE INTERACTION

In the general case, the integral (6) must be analyzed numerically. However, in the case where the dimensions of the interaction region V are small enough compared to the distance from the sources to the interaction region, so that the curvature of the primary spherical fronts can be neglected within it, an analytic solution can be found. In other words, this is the case of plane-wave interaction.

Assume V to be sufficiently small. Then slowly changing amplitude factors in the integrand of Eq. (6) can be taken out of the integral. Also, square roots like $R=[(x-x')^2+(y-y')^2+(z-z')^2]^{1/2}$, etc. can be developed in a series, and we can keep only linear terms with respect to r'/r. The quantitative criterion for applicability of these manipulations is given by

$$r'\ll(\lambda R_0^{\min})^{1/2}, \tag{7}$$

where λ is the minimum primary wavelength and $R_0^{\min}$ is the minimum distance from the sources to the points in the interaction region.

The above manipulations significantly simplify the integrand in Eq. (6). Assuming that the interaction region has the form of a parallelepiped, that the origin and observation point are both located in the (x,z) plane, and that the observation point is in the far field of DFW ($K\_R\gg 1$), we can rewrite the solution (6) in the following form:

$$u_x(r,\varphi,t)=-\frac{F_0^2 f_1 f_2 V}{8\pi\mu^2\rho c_l^2 c_t^2}\frac{m+n\cos^2\theta}{R_0 R_0^{(2)}}\sin\varphi\left(\frac{k_2}{R_0^{(2)}}-\frac{k_1}{R_0}-\frac{1}{r}(\delta'\cos\varphi+\epsilon'\sin\varphi)\right)$$
$$\times\frac{\sin[(a/\lambda_-)\pi\cos\varphi+(a/2)\delta']\sin[(c/\lambda_-)\pi\sin\varphi+(c/2)\epsilon']}{[(a/\lambda_-)\pi\cos\varphi+(a/2)\delta'][(c/\lambda_-)\pi\sin\varphi+(c/2)\epsilon']}$$
$$\times\sin[-k_1R_0+k_2R_0^{(2)}-2\pi(f_1-f_2)(r/c_t-t)],$$
$$\delta'=\frac{2\pi}{c_l}\left(-\frac{f_2}{R_0^{(2)}}(x_0+L)+\frac{f_1}{R_0}x_0\right),\quad \epsilon'=\frac{2\pi z_0}{c_l}\left(-\frac{f_2}{R_0^{(2)}}+\frac{f_1}{R_0}\right), \tag{8}$$

where R_0 and $R_0^{(2)}$ are the distances from the sources to the origin located at the center of parallelepiped, x_0 and z_0 are the coordinates of the vector $\mathbf{R}_0$, a and c are the parallelepiped sides, parallel to the x and z axes, respectively; c_l is the longitudinal wave velocity, ρ is the density, λ_- is the DFW wavelength, φ is the angle between the vector $\mathbf{r}$ and the z axis, and θ is the angle between the vectors $\mathbf{R}_0$ and $\mathbf{R}_0^{(2)}$.

The displacement in Eq. (8) is the difference-frequency wave displacement in the x direction, generated by two plane intersecting longitudinal sound beams.[1-3] Note that the amplitude of the scattered wave is proportional to the primary frequencies, the squared amplitude of the force developed by the sources, the volume of the interaction region, and the nonlinear elastic constants of the material. The angular factor in Eq. (8) depending on φ describes the directivity of the scattered wave in the (x,z) plane. A characteristic feature of the scattered wave directivity pattern is that the DFW radiation is summed up coherently in the direction defined by the synchronism conditions. Coherent summation of the elementary secondary sources causes the proportionality of the DFW amplitude to V. It can be shown by straightforward calculation that the direction of a main lobe of the directivity pattern given by the angular factor in Eq. (8) coincides with the direction determined by synchronism conditions.

III. THE GENERAL INTERACTION CASE

When the maximum dimension of the interaction region does not satisfy condition (7), the curvature of the primary fronts cannot be neglected, and the integral in Eq. (6) must be analyzed numerically.

In the numerical example given below, we use values of the parameters in Eq. (6) that are typical for exploration seismology experiment: $L=600$ m, $f_1=50$ Hz, $f_2=70$ Hz, $F_0=500$ kN, $c_l=3000$ m/s, $c_t=1500$ m/s, $\rho=2000$ kg/m^3; and the values for $m/\rho c_l^2$ and $n/\rho c_l^2$, which are the analogs of the nonlinear parameter for this type of interaction, are equal to 10^3. Note that nonlinear parameters for earth materials can have values up to 10^4 ([12]). To simplify the numerical integration, the interaction region was taken to be a cube with its center located symmetrically between the sources (Fig. 2). The depth of the center d was taken to be 1000 m.

The geometry used in a numerical example is selected such that the center of the interaction region is a point where synchronism conditions for primary wave vectors are satisfied exactly. This means that the angle between vectors connecting points O_1 and O, and O_2 and O in Fig. 2 is defined by the expression[1]

$$\cos\theta=1/q_2^2+[(q_2^2-1)(q_1^2+1)/2q_1q_2^2], \tag{9}$$

where $q_1=f_2/f_1$ and $q_2=c_t/c_l$.

Strictly speaking, the interaction is out of synchronism at every point except for the center of the region, because of the sphericity of interacting fronts. In the case of small V, the interaction can be considered approximately resonant, but for large V it is no longer resonant. In our calculations, we consecutively increased the volume of interaction, beginning with small V satisfying the condition (7), and increasing V to sizes significantly exceeding this limit, as shown in Fig. 2, so that the influence of sphericity on the resonance interaction could be studied. Amplitudes and directivity patterns of the DFW were calculated within a circle of radius 1000 m.

Figure 3 shows the calculated directivity patterns $u_x(\varphi)/u_x^{\max}(\varphi)$ of the DFW in the (x,z) plane. Figure

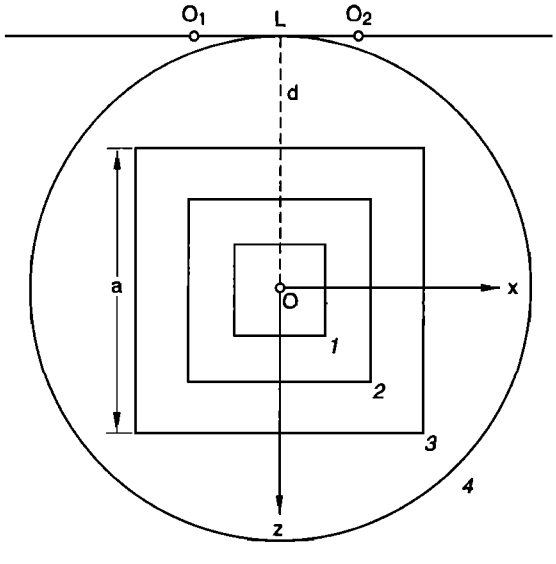

FIG. 2. Geometry used in numerical example. Here, a is side of the cube, d is depth of a center of the cube, 1–3 show consecutively increasing size of interaction volume, 4 is a circle on which the amplitudes and directivity patterns of DFW are calculated.

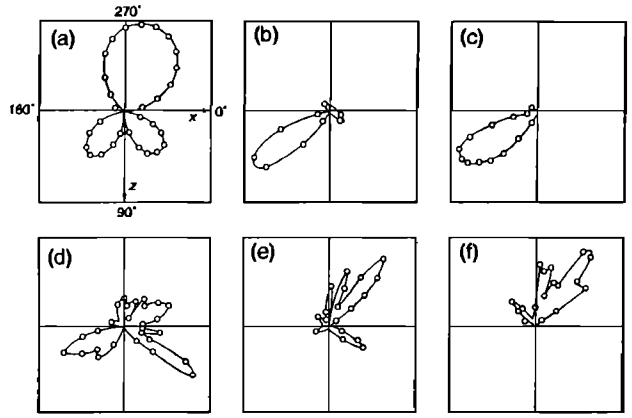

FIG. 3. Directivity patterns of the difference-frequency wave calculated for different sizes of interaction volume: (a)—$a=(1/3)\lambda_-$, (b)—$2\lambda_-$, (c)—$(16/3)\lambda_-$, (d)—$(22/3)\lambda_-$, (e)—$(28/3)\lambda_-$, (f)—$(56/3)\lambda_-$, where a is the cube side and λ_- is the DFW wavelength.

3(a)–(f) corresponds to increasing the size of the interaction volume. The maximum dimension in Fig. 3(a) and (b) satisfies the criterion of Eq. (7), so that the plane-wave approximation can be applied, and numerically calculated directivity patterns coincide with the results of calculation using asymptotic formula (8). Figure 3(a) has a quasiomnidirectional directivity pattern, because the interaction volume is so small that it can be considered a point source (cube side $a=\lambda_-/3$). Directional radiation is formed in Fig. 3(b), where the main lobe is oriented in the direction of synchronism ($a=2\lambda_-$). Figure 3(c)–(f) corresponds to the interaction volumes that no longer satisfy the criterion (7), and the form of the directivity patterns is affected by the sphericity of interacting waves. In Fig. 3(c) [$a=(16/3)\lambda_-$] the angular width of the main lobe does not decrease, compared with Fig. 3(b), as it should be for the plane wave case, and Fig. 3(d) [$a=(22/3)\lambda_-$] already shows a significant deviation of the radiation direction from the plane-wave radiation direction. New lobes appear as well. Further increasing the interaction volume, the DFW radiation concentrates in the direction defined approximately by the angle 310° [Fig. 3(e) and (f), $a=(28/3)\lambda_-$ and $(56/3)\lambda_-$, respectively]. Calculations for larger V showed that this latter direction is stable and does not change (increasing of interaction volume was limited, of course, by the requirement that it must have remained in the far field of sources).

Figure 4 shows the amplitude of the x component of the DFW field versus the volume of interaction in the synchronism direction (a) and in the 310° direction (b). Curve (a) shows that the amplitude in the synchronism direction grows linearly with volume, in accordance with Eq. (8), while the approximation of plane interacting waves holds. Then amplitude growth stops. Amplitude of radiation in 310° direction is two orders of magnitude weaker for small interaction volumes, but increases rapidly when the interaction volumes are large. This spatial direction corresponds to a stable summation of quasicoherent secondary sources, when the region is large and the influence of sphericity is significant.

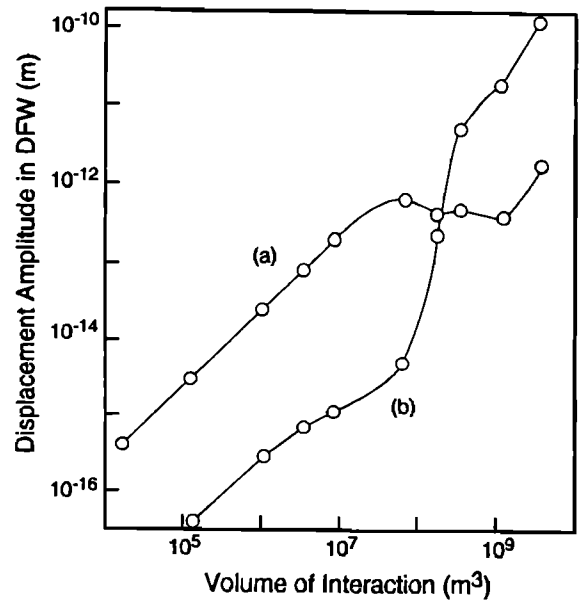

FIG. 4. Amplitude of the x component of the difference-frequency wave particle displacement versus the volume of interaction (a) in the synchronism direction and (b) the direction of 310°, corresponding to a maximum radiation for large interaction volumes.

There is a question about the effect of the shape of the volume on the directivity of the scattered DFW wave. The calculations so far are limited to cubes. We can suppose from qualitative considerations that for volumes that are small compared with the DFW wavelength the effect of the shape is negligible, because the region of interaction can be regarded as the point-like source. On the other hand, for large volumes having many wavelengths on its linear dimension the characteristic features of the radiation pattern are formed in the bulk of the volume, and the presence of the corners of a cube can affect only minor details of the directivity pattern. However, an accurate statement could be made after numerical examination.

The existence of a limiting direction of the DFW radiation, which does not change as interaction volume increases, can be explained by the spherical spreading of the primary waves, whose amplitudes decrease as $1/R$. Remote zones of the interaction region do not affect the result of the interaction, because amplitudes of the primaries become very small there. Thus, characteristics of the DFW field are determined by a limited region of space, where intensities of the secondary sources are the largest. This fact shows that in the real seismic experiments the characteristics of the recorded nonlinearly scattered field will be dominated by the integrated nonlinear properties of a spatially limited region of the Earth's crust. In these experiments the actual directivity of the primary vibratory sources will also contribute to the confining the interaction volume.

IV. DISCUSSION AND CONCLUSIONS

Figure 3(e) and (f) shows that the main lobe of the DFW radiation has a "backward" direction, since the primary sources are at the top of (x,z) plane. Thus, the in-

teraction of spherical waves on large nonlinear inhomogeneities leads to a backscattered transverse difference-frequency wave. The amplitude of the backscattered wave reaches the value of 10^{-10}–10^{-9} m (Fig. 4), for the values of parameters used in the numerical example. These conditions could be reconstructed in a real field experiment. The above amplitude of the DFW is equal to amplitudes of weak microseismic noise, implying that nonlinearly scattered radiation can be realistically recorded.

Due to the fact that the interaction region for spherical waves is localized in space, and that the DFW-radiation amplitude is proportional to its nonlinear parameter, this type of nonlinear interaction could be used in remote sensing of nonlinear properties of the Earth's crust. If vibratory sources of seismic waves are employed, the depth of the interaction region can be altered by changing distance between sources. The values of nonlinear parameters at different depths would provide valuable information about the physical state of the *in situ* rock.

ACKNOWLEDGMENTS

I would like to thank A. V. Nikolaev from the Institute of Physics of the Earth in Moscow, G. M. Shalashov from the Radiophysics Research Institute in Nizhniy Novgorod (formerly Gorky), Russia, B. Ya. Gurevich from the VNIIGeosystems Institute in Moscow, and P. A. Johnson from the Los Alamos National Laboratory, USA, for the discussions and suggestions that largely helped in the fulfillment of this work. Katherine McCall of Los Alamos Laboratory carefully read the manuscript and suggested significant improvements. I appreciate the recommendations of the reviewer of this paper. My special thanks is to Ruth Bigio for preparing the illustrations.

[1] G. L. Jones and R. D. Kobett, "Interaction of Elastic Waves in an Isotropic Solid," J. Acoust. Soc. Am. **35**, 5–10 (1963).

[2] J. D. Childress and C. G. Hambrick, "Interactions Between Elastic Waves in an Isotropic Solid," Phys. Rev. A **136**, A411–A418 (1964).

[3] L. H. Taylor and F. R. Rollins, Jr., "Ultrasonic Study of Three-Phonon Interactions. I. Theory," Phys. Rev. A **136**, A591–A596 (1964).

[4] F. R. Rollins, Jr., "Interaction of Ultrasonic Waves in Solid Media," Appl. Phys. Lett. **2**, 147–148 (1963).

[5] H.-F. Kun, L. K. Zarembo, and V. A. Krasil'nikov, "Experimental Investigation of Combination Scattering of Sound by Sound in Solids," Sov. Phys. JETP **21**, 1073–1077 (1965).

[6] P. A. Johnson, T. J. Shankland, R. J. O'Connell, and J. N. Albright, "Nonlinear Generation of Elastic Waves in Crystalline Rock," J. Geophys. Res. **92** (B5), 3597–3602 (1987).

[7] P. A. Johnson and T. J. Shankland, "Nonlinear Generation of Elastic Waves in Granite and Sandstone: Continuous Wave and Travel Time Observations," J. Geophys. Res. **94**(B12), 17 729–17 733 (1989).

[8] G. M. Shalashov, "An Estimation of the Possibility of Nonlinear Vibrational Seismic Prospecting," Izv. Acad. Sci. USSR, Fiz. Zemli (Physics of the Solid Earth) **21**, 234–235 (1985).

[9] I. A. Beresnev, A. V. Nikolayev, V. S. Solov'yev, and G. M. Shalashov, "Nonlinear Phenomena in Seismic Surveying Using Periodic Vibrosignals," Izv. Acad. Sci. USSR, Fiz. Zemli (Physics of the Solid Earth) **22**, 804–811 (1986).

[10] I. A. Beresnev and A. V. Nikolaev, "Experimental Investigations of Nonlinear Seismic Effects," Phys. Earth Plan. Int. **50**, 83–87 (1988).

[11] B. P. Bonner and B. J. Wanamaker, "Acoustic Nonlinearities Produced by a Single Macroscopic Fracture in Granite," in *Review of Progress in Quantitative Nondestructive Evaluation*, edited by D. O. Thompson and D. E. Chimenti (Plenum, New York, 1991), pp. 1861–1867.

[12] L. A. Ostrovsky, "Wave Processes in Media With Strong Acoustic Nonlinearity," J. Acoust. Soc. Am. **90**, 3332–3337 (1991).

[13] L. D. Landau and E. M. Lifshitz, *Theory of Elasticity* (Pergamon, New York, 1986), pp. 104–107.

[14] Z. A. Gol'dberg, "Interaction of Plane Longitudinal and Transverse Elastic Waves," Sov. Phys. Acoust. **6**, 306–310 (1960).

[15] G. F. Miller and H. Pursey, "On the Partition of Energy Between Elastic Waves in a Semi-Infinite Solid," Proc. R. Soc. London, Ser. A **233**, 55–69 (1955).